


A designed cyclic analogue of gomesin has potent activity against *Staphylococcus aureus* biofilms

Susana A. Dias¹, Sandra N. Pinto^{2,3}, Ana S. Silva-Herdade¹, Olivier Cheneval⁴, David J. Craik ⁴, Ana Coutinho^{2,3,5}, Miguel A. R. B. Castanho¹, Sónia T. Henriques^{4,6} and Ana Salomé Veiga^{1*}

¹Instituto de Medicina Molecular, Faculdade de Medicina, Universidade de Lisboa, Av. Prof. Egas Moniz 1649-028 Lisboa, Portugal; ²iBB-Institute for Bioengineering and Biosciences, Department of Bioengineering, Instituto Superior Técnico, Universidade de Lisboa, Av. Rovisco Pais 1049-001 Lisboa, Portugal; ³Associate Laboratory i4HB — Institute for Health and Bioeconomy at Instituto Superior Técnico, Universidade de Lisboa, Av. Rovisco Pais, 1049-001 Lisboa, Portugal; ⁴Institute for Molecular Bioscience, Australian Research Council Centre of Excellence for Innovations in Peptide and Protein Science, The University of Queensland, Brisbane, QLD, 4072 Australia; ⁵Departamento de Química e Bioquímica, Faculdade de Ciências, Universidade de Lisboa, Campo Grande 1749-016 Lisboa, Portugal; ⁶School of Biomedical Sciences, Queensland University of Technology, Translational Research Institute, Australian Research Council Centre of Excellence for Innovations in Peptide and Protein Science, Brisbane, QLD, 4102 Australia

*Corresponding author. E-mail: aveiga@medicina.ulisboa.pt

Received 13 April 2022; accepted 18 August 2022

Background: Infections caused by bacterial biofilms are very difficult to treat. The use of currently approved antibiotics even at high dosages often fails, making the treatment of these infections very challenging. Novel antimicrobial agents that use distinct mechanisms of action are urgently needed.

Objectives: To explore the use of [G1K,K8R]cGm, a designed cyclic analogue of the antimicrobial peptide gomesin, as an alternative approach to treat biofilm infections.

Methods: We studied the activity of [G1K,K8R]cGm against biofilms of *Staphylococcus aureus*, a pathogen associated with several biofilm-related infections. A combination of atomic force and real-time confocal laser scanning microscopies was used to study the mechanism of action of the peptide.

Results: The peptide demonstrated potent activity against 24 h-preformed biofilms through a concentration-dependent ability to kill biofilm-embedded cells. Mechanistic studies showed that [G1K,K8R]cGm causes morphological changes on bacterial cells and permeabilizes their membranes across the biofilm with a half-time of 65 min. We also tested an analogue of [G1K,K8R]cGm without disulphide bonds, and a linear unfolded analogue, and found both to be inactive.

Conclusions: The results suggest that the 3D structure of [G1K,K8R]cGm and its stabilization by disulphide bonds are essential for its antibacterial and antibiofilm activities. Moreover, our findings support the potential application of this stable cyclic antimicrobial peptide to fight bacterial biofilms.

Introduction

Biofilms comprise aggregates of bacterial cells encased in a matrix of self-produced extracellular polymeric substances (EPS), e.g. polysaccharides, proteins and extracellular DNA (eDNA).^{1,2} These biofilms are responsible for many chronic and persistent infections that occur in the human body, such as lung infections in cystic fibrosis patients or chronic wound infections,^{3–5} and are frequently involved in medical device-associated infections.^{6,7} The treatment of these infections is often difficult as

biofilm-embedded bacteria can escape the host immune system and are more tolerant to conventional antibiotics than bacteria in the planktonic form.³ Tolerance mechanisms include the reduced diffusion or sequestration of antibiotics in the EPS matrix, and the slow growth rate of biofilm-embedded cells that hinders antibiotic activity, as they usually target metabolic active processes. Novel antimicrobial agents that are active against bacterial biofilms are urgently needed and antimicrobial peptides (AMPs) are a promising option.^{8,9} Although AMPs are a diverse group of molecules, most have short amino acid sequences, a high

content of cationic and hydrophobic residues, and broad-spectrum activity.^{10,11} Furthermore, their main mechanism of action involves the disruption of bacterial membranes,¹² giving them the ability to kill slow-growing and non-growing bacteria in biofilms.

Gomesin (Gm) is a cationic 18-residue AMP originally isolated from the haemocytes of the Brazilian spider *Acanthoscurria gomesiana*.¹³ Structurally, the peptide consists of a β -hairpin, where two antiparallel β -strands are connected by a loop and stabilized by two disulphide bonds (Cys2-15 and Cys6-11) in a parallel arrangement,¹⁴ which are crucial for its antimicrobial activity and resistance to serum proteases.^{15,16} Gm is also known for its anticancer,¹⁷ antimalarial,¹⁸ anticryptococcal¹⁹ and anti-*Leishmania*²⁰ activity. Mechanistic studies suggest that the activity of the peptide is, at least partially, dependent on its ability to interact and permeabilize anionic lipid membranes.²¹ Mattei et al.²² showed that the primary interaction of Gm with membranes depends on surface electrostatic interactions, and the insertion of the hydrophobic portion into the membrane is responsible for permeabilization.

Head-to-tail cyclization of bioactive peptides is a promising approach for improving their activity^{23,24} and resistance to serum proteases,²⁵ as conformational constraints enhance their binding and selectivity towards the target, as well as their stability.²⁶ Several studies have shown that cyclic peptides have increased antimicrobial activity compared with their linear analogues.²⁷⁻²⁹ For example, the cyclic peptide labaditin, derived from the plant *Jatropha multifida*, revealed strong activity against planktonic *Staphylococcus aureus*, in contrast to its linear analogue that was ineffective, indicating that its cyclic structure is essential for antimicrobial activity.²⁷ In another study, it was shown that cyclization of the peptide cryptdin-4 (Cp4), an α -defensin with a triple-stranded antiparallel β -sheet, resulted in improved antimicrobial activity against several Gram-positive and Gram-negative bacteria compared with the native peptide, while maintaining a low haemolytic activity and high stability in human serum.³⁰

In the case of a cyclic analogue of gomesin, cGm, backbone cyclization increased serum stability and enhanced anticancer and antimalarial activities when compared with the native peptide, but no significant improvement in the activity against *Escherichia coli* was observed.³¹ However, the rationally designed cGm analogue,³² [G1K,K8R]cGm (Figure 1a), exhibits a 10-fold increase in potency against Gram-positive and Gram-negative bacteria, compared with native Gm or cGm (e.g. MIC against *S. aureus* is 32 μ M for cGm and 2 μ M for [G1K,K8R]cGm), while maintaining high stability in serum and low haemolytic activity ($HC_{50} > 64 \mu$ M).³² This peptide was obtained by replacing Gly1 with Lys, and Lys8 with Arg, and has a net charge of +7, whereas cGm has a net charge of +6, at pH 7.4. Mechanistic studies showed that the antimicrobial activity of [G1K,K8R]cGm is dependent on its ability to bind and disrupt the bacterial membrane after penetrating the outer protective layer.³²

Despite the demonstrated potential of Gm and its cyclic analogues against bacteria in the planktonic form, to the best of our knowledge there are no studies on their activity against bacterial biofilms. In the present study, we show that the cGm analogue [G1K,K8R]cGm has potent activity against biofilms of *S. aureus*, a Gram-positive bacterium frequently associated with biofilm-

related infections.^{33,34} Using a combination of atomic force and confocal laser scanning microscopies we found that the mechanism of action of the peptide involves membrane disruption of biofilm-embedded cells. In addition, using a backbone cyclized analogue without disulphide bonds ([G1K,K8R]cGm-reduced, Figure 1b), and a linear and unfolded analogue (lin[G1K,K8R]cGm, Figure 1c), we were able to demonstrate the importance of the [G1K,K8R]cGm folding for its antibacterial and antibiofilm activities.

Methods

Peptide synthesis, folding and purification

Peptides were assembled using Fmoc solid-phase chemistry on 2-chlorotrityl chloride resin. [G1K,K8R]cGm³² was synthesized, cyclized and folded using methodology reported by Cheneval et al.³⁵ Disulphide bond formation and correct connectivity was confirmed using 1D ¹H NMR spectroscopy (Figure S1, available as Supplementary data at JAC Online) on a Bruker Avance 600 MHz spectrometer (Billerica, USA).³¹ The backbone cyclized analogue without disulphide bonds, [G1K,K8R]cGm-reduced, and the linear analogue, lin[G1K,K8R]cGm, have the four Cys (Cys2, 6, 11 and 15) of [G1K,K8R]cGm replaced with the unnatural amino acid L-2-aminobutyric acid. Analysis of the 1D NMR spectra of these two analogues showed poor separation of resonance signals (Figure S1), suggesting that both are unstructured. The masses of the peptides were confirmed using electrospray ionisation mass spectrometry (Table S1) and both peptides were $\geq 95\%$ pure, as confirmed by reversed-phase HPLC (RP-HPLC) (Figure S2). To prepare stock solutions, lyophilized peptides were weighed out on a high-precision analytical microbalance, dissolved in sterile Milli-Q water and peptide concentration was determined by absorbance at 280 nm (Table S1). Aliquots were stored at -20°C .

Bacterial strain and growth conditions

S. aureus strain ATCC 6538 was purchased from ATCC (Manassas, VA, USA). *S. aureus* planktonic bacteria were grown in Mueller-Hinton Broth (MHB) (BD, Franklin Lakes, NJ, USA), for 18 h, at 37°C . *S. aureus* bacterial biofilms were grown in tryptic soy broth (TSB) (BD) containing 0.25% (w/v) glucose (TSBG) (Sigma-Aldrich, St. Louis, MO, USA), for 24 h, at 37°C , to allow biofilm formation.

Activity against planktonic bacteria

The ability of [G1K,K8R]cGm, [G1K,K8R]cGm-reduced and lin[G1K,K8R]cGm to inhibit bacterial growth was evaluated by determining the MIC using a standard broth microdilution procedure,^{36,37} as previously described.³⁸ *S. aureus* suspensions were prepared in MHB to a final concentration of 1×10^6 cfu/mL and incubated for 18 h at 37°C in a sterile 96-well microtitre round-bottomed polypropylene plate (Corning, NY, USA), containing 2-fold dilutions of each peptide. Final bacterial concentration was 5×10^5 cfu/mL, whereas peptide concentration ranged from 0.78 to 100 μ M. The MIC was defined as the lowest peptide concentration required to inhibit visible bacterial growth.

Activity against *S. aureus* biofilms

The antibiofilm activity of [G1K,K8R]cGm against 24 h-preformed *S. aureus* biofilms was evaluated using three distinct methods, as previously described:³⁹ a resazurin reduction fluorometric assay and a colony count assay to determine the metabolic activity and viability of biofilm-embedded cells, respectively; and a crystal violet assay to quantify the total biofilm biomass.

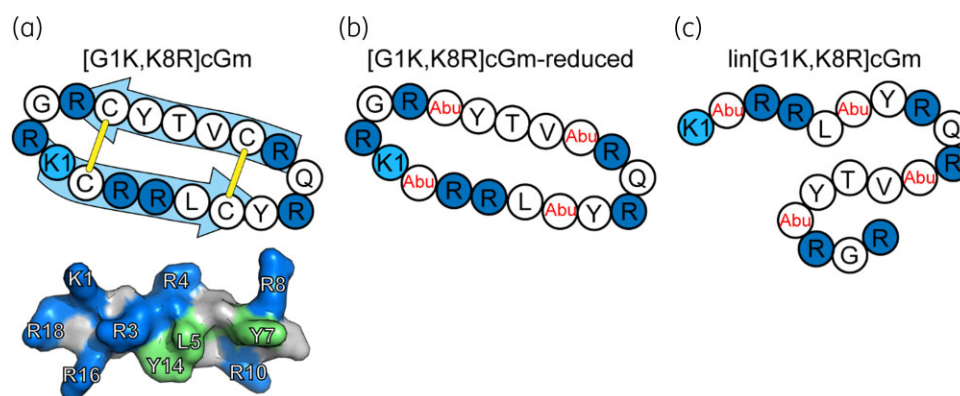


Figure 1. Schematic representation of [G1K,K8R]cGm (a), [G1K,K8R]cGm-reduced (b) and lin[G1K,K8R]cGm (c). The sequence diagram of [G1K,K8R]cGm (a, top panel) shows the two antiparallel β -strands (light blue arrows) and the two parallel disulphide bonds between Cys2-15 and Cys6-11 (yellow sticks). As shown in the surface representation of [G1K,K8R]cGm (A, bottom panel), positively charged residues (shown in blue) and Tyr residues (shown in green) are located in the same region of the peptide. The amino acid residues modified in [G1K,K8R]cGm-reduced (b) and lin[G1K,K8R]cGm (c) peptides are highlighted in red. The first amino acid residue (K1) and the positively charged residues (dark blue) are indicated in all the peptides. [G1K,K8R]cGm and [G1K,K8R]cGm-reduced are backbone cyclized, whereas lin[G1K,K8R]cGm has free N- and C-terminals. To prevent the formation of disulphide bonds in [G1K,K8R]cGm-reduced and lin[G1K,K8R]cGm, the four Cys (Cys2, 6, 11 and 15) of [G1K,K8R]cGm were replaced with the unnatural amino acid L-2-aminobutyric acid (presented as Abu). The net charge of these peptides at pH 7.4 is +7. This figure appears in colour in the online version of JAC and in black and white in the print version of JAC.

Resazurin reduction fluorometric assay

S. aureus suspensions at 1×10^6 cfu/mL were incubated in a sterile 96-well microtitre black flat-bottomed polystyrene plate (Corning) for 24 h at 37°C. After a washing step with MHB to remove non-adherent bacteria, preformed biofilms were incubated in the absence or presence of 2-fold serial dilutions of [G1K,K8R]cGm, ranging from 0.78 to 50 μ M, for 4 or 24 h at 37°C, or with [G1K,K8R]cGm-reduced and lin[G1K,K8R]cGm, ranging from 0.78 to 50 μ M, for 4 h at 37°C. The antibiotic vancomycin (Sigma–Aldrich) was also tested from 2.07 to 69 μ M. Untreated biofilms were used as a control. After washing the biofilms twice with MHB, alamarBlue® reagent (Invitrogen, Carlsbad, CA, USA) was added at a final concentration of 10% (v/v in MHB) to each sample and its reduction was monitored by measuring the fluorescence intensity (excitation and emission wavelengths were 530 and 590 nm, respectively) of the samples every 5 min during 2 h at 37°C, in an Infinite® M200 microplate reader (Tecan, Männedorf, Switzerland). Resazurin, the active compound in alamarBlue® reagent, is a blue dye that can be reduced to a pink fluorescent intermediate, resorufin, as a result of the metabolic activity of cells.⁴⁰ Fully reduced resazurin (i.e. resorufin) in MHB, obtained after autoclaving the sample for 15 min, was used as positive control. The percentage of resazurin reduction was determined relatively to the control, after blank (10% v/v alamarBlue® reagent in MHB) correction.

Colony count assay

S. aureus suspensions at 1×10^6 cfu/mL were incubated in a 96-well microtitre clear flat-bottomed polystyrene plate (Corning) for 24 h at 37°C. After a washing step with MHB to remove non-adherent bacteria, preformed biofilms were incubated in the absence or presence of 2-fold serial dilutions of [G1K,K8R]cGm, ranging from 0.78 to 50 μ M, for 4 h at 37°C. Untreated biofilms were used as a control. After washing the biofilms twice with sterile PBS (pH 7.4), the biofilms were resuspended in PBS, followed by cell scrapping with a pipette tip as described elsewhere.^{41,42} Aliquots were vortexed at high speed, serially diluted in PBS and plated on nutrient-rich Trypticase soy agar (TSA) plates (bioMérieux, Marcy l'Étoile, France). After incubation for 24 h at 37°C, bacterial colonies were counted, and viable bacteria (in cfu/mL) were reported as percentage of the control.

Crystal violet binding assay

Crystal violet is a basic dye that binds to negatively charged molecules, such as those in biofilm EPS matrix and on bacterial membrane surface,⁴³ thus staining the biofilm biomass. *S. aureus* suspensions at 1×10^6 cfu/mL were incubated in a 96-well microtitre clear flat-bottomed polystyrene plate (Corning) for 24 h at 37°C. After a washing step with MHB to remove non-adherent bacteria, preformed biofilms were incubated in the absence or presence of 2-fold serial dilutions of [G1K,K8R]cGm, ranging from 0.78 to 50 μ M, for 4 h at 37°C. Untreated biofilms were used as a control. Biofilms were washed twice with MHB and incubated with 0.25% (v/v) crystal violet (Sigma–Aldrich) in sterile Milli-Q water, for 30 min at room temperature. After washing each sample three times with MHB, crystal violet was solubilized with 95% (v/v) ethanol (Carlo Erba Reagents S.A.S., France) by repeated pipetting. Biofilm biomass was quantified by measuring the absorbance at 590 nm of each sample in an Infinite® M200 microplate reader (Tecan). The percentage of crystal violet staining was determined relatively to the control, after blank [0.25% (v/v) crystal violet in sterile Milli-Q water] correction.

Biofilm imaging methods

Atomic force microscopy (AFM) and confocal laser scanning microscopy (CLSM) were used to visualize the effect of [G1K,K8R]cGm and lin[G1K,K8R]cGm on *S. aureus* biofilms. Details on these methods are provided as Supplementary data.

Results and discussion

[G1K,K8R]cGm has potent activity against preformed *S. aureus* biofilms

To determine the antibiofilm activity of [G1K,K8R]cGm, 24 h-preformed biofilms of *S. aureus* ATCC 6538 were used. Treatment of the preformed biofilms with increasing concentrations of [G1K,K8R]cGm, for either 4 or 24 h, resulted in a significant reduction of the metabolic activity of biofilm-embedded cells, as quantified by a resazurin fluorometric assay (Figure 2a), being even more potent than the antibiotic

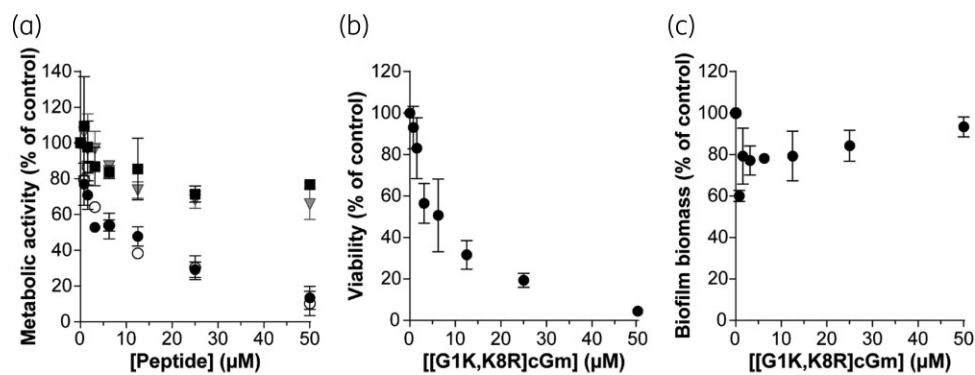


Figure 2. Effect of [G1K,K8R]cGm, [G1K,K8R]cGm-reduced and lin[G1K,K8R]cGm on *S. aureus* biofilms. (a) The metabolic activity of biofilm-embedded cells was evaluated using a resazurin reduction fluorometric assay after treatment with [G1K,K8R]cGm for 4 h (filled circles) or 24 h (open circles), or with [G1K,K8R]cGm-reduced (filled triangles) and lin[G1K,K8R]cGm (filled squares) for 4 h. (b) The viability of biofilm-embedded cells was evaluated using a colony count assay after treatment with [G1K,K8R]cGm for 4 h. (c) Biofilm biomass was evaluated using a crystal violet binding assay after treatment with [G1K,K8R]cGm for 4 h. In the three assays, percentages were determined relatively to the control (untreated biofilm).

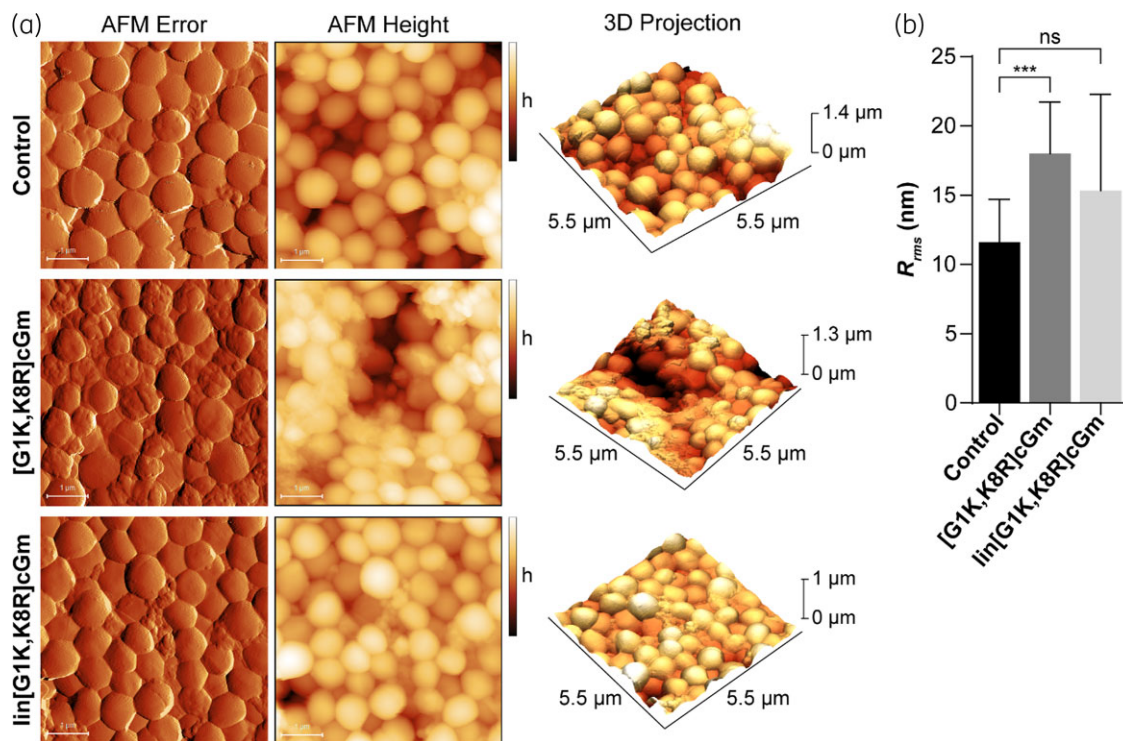


Figure 3. Effect of [G1K,K8R]cGm and lin[G1K,K8R]cGm on *S. aureus* biofilms imaged by AFM. (a) Representative AFM error and height images, and respective 3D projections, of untreated biofilms (top panel) and biofilms treated with 25 µM [G1K,K8R]cGm (middle panel) or lin[G1K,K8R]cGm (bottom panel), for 4 h. Total scanning area for each image was 5 × 5 µm. For 3D projections, the total scanning area was 5.5 × 5.5 µm. h, height. (b) R_{rms} of untreated and peptide-treated biofilms. Ns, non-significant; *** P value ≤ 0.001 . This figure appears in colour in the online version of *JAC* and in black and white in the print version of *JAC*.

vancomycin (Figure S3). This effect was dependent on the peptide concentration, but not on the incubation time. Moreover, the treatment of biofilms with peptide for 4 h, resulted in a significant reduction of the viability of bacterial cells, as shown with a colony count assay (Figure 2b). Specifically, treatment with 50 µM [G1K,K8R]cGm, the highest concentration tested, reduced the metabolic activity of preformed biofilms by ~90% and the cell viability by ~96%, suggesting that the peptide kills

biofilm-embedded bacteria. The results also showed that the peptide had a small impact on the biofilm biomass (Figure 2c), evaluated using a crystal violet assay. Since bacterial cells account for less than 10% of the dry mass,² the results corroborate the hypothesis that the peptide acts mainly at cell level.

[G1K,K8R]cGm has an amphipathic structure, in which hydrophobic residues form a small hydrophobic patch on the surface of the molecule surrounded by positively charged residues forming

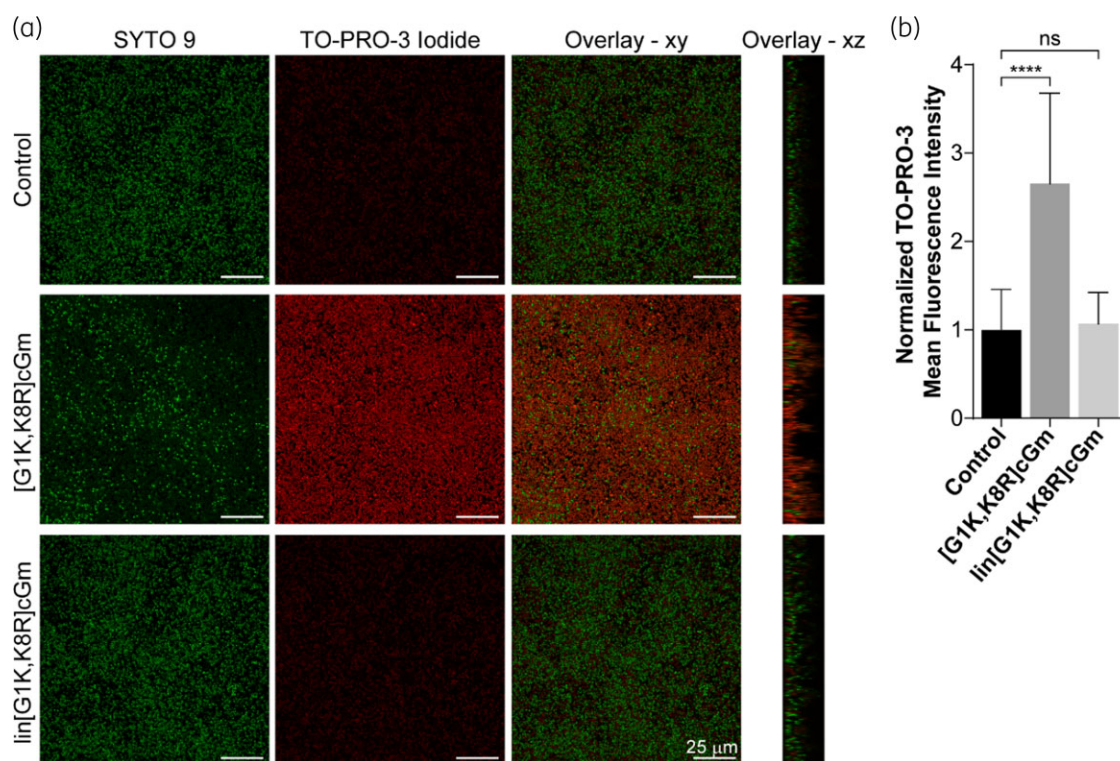


Figure 4. Effect of [G1K,K8R]cGm and lin[G1K,K8R]cGm on the membrane integrity of *S. aureus* biofilm-embedded cells imaged by CLSM. (a) Representative CLSM images of untreated biofilms (top panels) and biofilms treated with 25 μM [G1K,K8R]cGm (middle panels) or lin[G1K,K8R]cGm (bottom panels), for 4 h. Biofilms were stained with the nucleic acid-binding dyes SYTO 9 (green) and TO-PRO-3 iodide (red). The overlay between the green and red channels from the xy and xz orthogonal plane images are presented. The xy plane images were taken at an inner layer of the biofilms ($z = 2 \mu\text{m}$). (b) Normalized TO-PRO-3 mean fluorescence intensity for untreated, [G1K,K8R]cGm-treated and lin[G1K,K8R]cGm-treated biofilms. ns, non-significant; **** P value ≤ 0.0001 . This figure appears in colour in the online version of JAC and in black and white in the print version of JAC.

a charged patch (Figure 1a). This amphipathic organization is likely to be important for its membrane-binding properties and antimicrobial potency, as supported by studies with cGm analogues with mutations in hydrophobic and/or positively charged residues.³² The amphipathic properties and overall 3D structure of [G1K,K8R]cGm are maintained by a backbone cyclization and two disulphide bonds. To evaluate the importance of the 3D organization of [G1K,K8R]cGm in its antibiofilm activity, a backbone cyclized analogue without disulphide bonds, [G1K,K8R]cGm-reduced, and a linear unfolded analogue (i.e. not backbone cyclized and without disulphide bonds), lin[G1K,K8R]cGm, were studied. In both analogues, the four Cys residues present in [G1K,K8R]cGm, at positions 2, 6, 11 and 15, were replaced with the unnatural amino acid L-2-aminobutyric acid (Figure 1b and c). This amino acid has structural similarities with cysteine, but it has a methyl group instead of a thiol on the side chain, rendering it unable to form disulphide bonds.

The results showed that both [G1K,K8R]cGm-reduced and lin[G1K,K8R]cGm have a limited effect on the metabolic activity of biofilm-embedded cells when compared with the parent peptide (Figure 2a). Similar results were obtained when the peptides were tested against bacteria in the planktonic form, with MIC values of 3.13, >50 and >100 μM for [G1K,K8R]cGm, [G1K,K8R]cGm-reduced and the linear unfolded analogue, respectively. Although we cannot exclude the potential role of cysteine

residues for the antimicrobial activity of [G1K,K8R]cGm, as proposed for other peptides,^{44,45} these results suggest that the folding of [G1K,K8R]cGm and its stabilization by the disulphide bonds are required for its antibacterial and antibiofilm activity. Similar observations were obtained with a cyclic antimicrobial peptide with comparable 3D structure:⁴⁶ the linear unfolded analogue was inactive. However, for the backbone cyclized analogue without disulphide bonds the results were different, since although a reduced antibacterial activity was observed, it was not completely abrogated as in the case of the [G1K,K8R]cGm-reduced analogue.

[G1K,K8R]cGm affects the morphology and topography of biofilm-embedded bacterial cells

AFM was used to directly visualize changes on the morphology and topography of biofilm-embedded bacterial cells^{47,48} induced by [G1K,K8R]cGm on *S. aureus* biofilms. Representative AFM error and height images, and the correspondent 3D projection of untreated biofilms (Figure 3a, top panels), show a dense and uniform layer of cells with a characteristic staphylococcal round shape, as well as a smooth surface. In contrast, the images obtained after treatment of the biofilms with 25 μM [G1K,K8R]cGm for 4 h (Figure 3a, middle panels), clearly show changes on the morphology of the bacterial cells, which became more

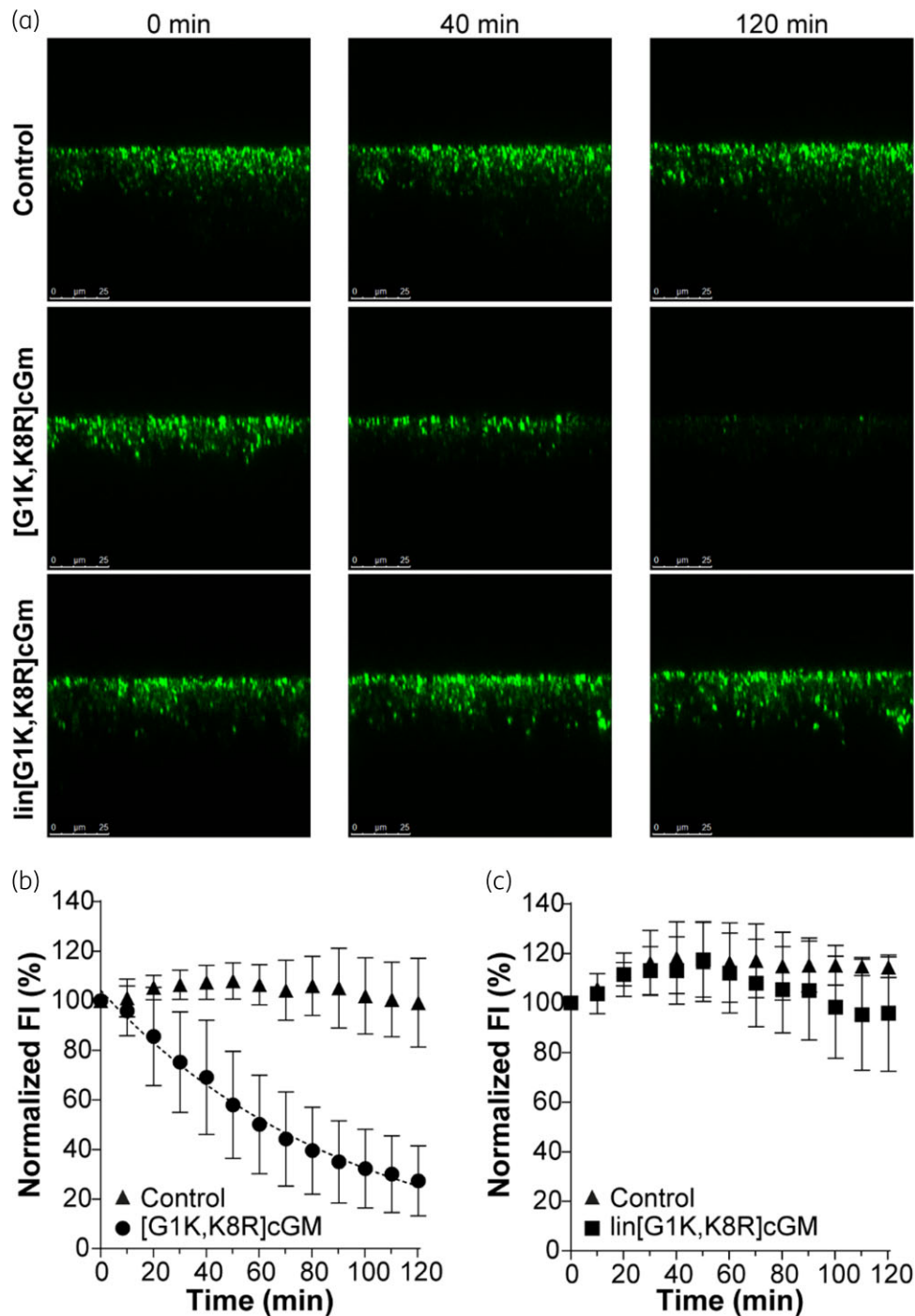


Figure 5. Effect of [G1K,K8R]cGm and lin[G1K,K8R]cGm on biofilm-embedded cells followed by a time-lapsed CLSM-based assay. (a) Representative CLSM images of untreated biofilms (top panels) and biofilms treated with 25 μM [G1K,K8R]cGm (middle panels) or lin[G1K,K8R]cGm (bottom panels). Biofilms were stained with the dye calcein (green). (b–c) Calcein fluorescence intensity (FI) from a pre-defined ROI was measured over time for untreated, [G1K,K8R]cGm-treated and lin[G1K,K8R]cGm-treated biofilms. A monoexponential decay curve (dashed line) was fitted by non-linear regression to the experimental data obtained for [G1K,K8R]cGm-treated biofilms. This figure appears in colour in the online version of JAC and in black and white in the print version of JAC.

irregular. In line with the antibiofilm activity results, no changes were observed on the bacterial cells of biofilms treated with 25 μM lin[G1K,K8R]cGm (Figure 3a, bottom panels), confirming the inability of this analogue to act against *S. aureus* biofilms.

To quantify the changes of the topography of the bacterial cells, the cell surface root mean square roughness (R_{rms}) was determined (Figure 3b). The R_{rms} value obtained for untreated biofilms was 11.6 ± 3.1 nm, increasing to 18.0 ± 3.7 nm after

treatment with 25 μM [G1K,K8R]cGm, quantitatively showing that the surface of biofilm cells becomes perturbed after treatment with the peptide. Treatment with 25 μM lin[G1K,K8R]cGm resulted in an R_{rms} of 15.3 ± 6.9 nm, a statistically non-significant difference, confirming the lack of changes on the topography noted in the qualitative image analysis.

[G1K,K8R]cGm kills biofilm-embedded bacterial cells through membrane permeabilization

To evaluate the ability of [G1K,K8R]cGm to permeate the membrane of biofilm-embedded bacteria, a CLSM-based assay was performed using 24 h-preformed *S. aureus* biofilms. Biofilms were sequentially stained with the nucleic acid-binding dyes SYTO 9 and TO-PRO-3 iodide. SYTO 9 permeates cells and binds to the intracellular DNA (iDNA) of all bacteria, having intact or damaged membranes, staining bacteria green, whilst TO-PRO-3 iodide only binds to the iDNA of bacteria with damaged membranes, staining bacteria red.^{49,50} Representative CLSM images obtained at an inner layer of untreated biofilms ($z=2$ μm) (Figure 4a, top panels) show the bacterial population stained green, thus having an intact membrane. Treatment of the biofilms with 25 μM [G1K,K8R]cGm for 4 h (Figure 4a, middle panels), resulted in an increase of the density of bacteria stained with TO-PRO-3 iodide and a concurrent decrease of bacteria stained with SYTO9 (left panels, SYTO9 and TO-PRO-3 iodide xy plane images). This suggests that TO-PRO-3 iodide enters into biofilm-embedded cells with peptide-induced compromised membranes. Once inside the cells, TO-PRO-3 iodide displaces, at least partially, the SYTO 9 bound to the iDNA, resulting in bacteria that appear orange in the xy and xz overlay images. In agreement, the quantitative analysis of the mean fluorescence intensity of TO-PRO-3 iodide at an inner layer of the biofilm ($z=2$ μm) (Figure 4b), shows a significant increase of the dye signal, demonstrating the ability of the peptide to disrupt the membrane of biofilm-embedded cells. These results agree with prior studies with [G1K,K8R]cGm,³² suggesting that its antimicrobial mode of action towards bacteria in the planktonic form is dependent on the ability to bind and disrupt the bacterial membrane. In contrast, for biofilms treated with lin[G1K,K8R]cGm (Figure 4a, bottom panels; and Figure 4b), no significant changes on TO-PRO-3 iodide fluorescence intensity were observed, showing that the linear analogue does not affect the membrane permeability of biofilm-embedded bacteria, as expected from the results above.

[G1K,K8R]cGm induces fast membrane permeabilization kinetics of biofilm-embedded bacterial cells

To investigate the kinetics of membrane permeation of [G1K,K8R]cGm we used a real-time CLSM-based assay of calcein release.³⁹ 24 h-preformed *S. aureus* biofilms were incubated with the cell-permeant and non-fluorescent dye calcein-AM for 3 h to allow its cellular uptake. Once inside the cytoplasm, calcein-AM is hydrolysed by intracellular esterases releasing calcein,^{51,52} a highly fluorescent compound that stains bacteria green. Damage of the membrane integrity of bacterial cells induces calcein release and dilution into the extracellular media, with a consequent decrease in its fluorescence emission intensity. Thus, a decrease in the

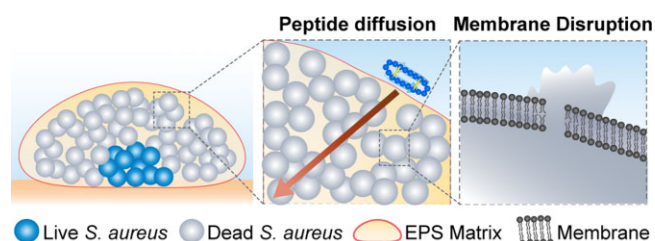


Figure 6. [G1K,K8R]cGm antibiofilm mechanism of action. The peptide is able to diffuse across the biofilm matrix and kill bacteria by targeting and disrupting their cell membranes. This figure appears in colour in the online version of JAC and in black and white in the print version of JAC.

calcein fluorescence emission intensity can be correlated with the permeabilizing effect of [G1K,K8R]cGm.

Representative CLSM images obtained for untreated and peptide-treated biofilms are shown in Figure 5a, while their quantitative analysis are shown in Figures 5b and c. The quantitative analysis was performed by evaluating the relative changes over time in the average fluorescence emission intensity from a rectangular region of interest (ROI) encompassing the calcein-stained biofilms. For both untreated biofilms and biofilms treated with lin[G1K,K8R]cGm, the average fluorescence emission intensity of calcein remained largely unchanged over the 2 h incubation. The slight increase observed was possibly due to a slow background hydrolysis of calcein-AM by the intact biofilm-embedded bacteria. For biofilms treated with 25 μM [G1K,K8R]cGm, a decrease of the average calcein fluorescence emission intensity was observed over the incubation time, as a consequence of the peptide permeabilizing bacterial membranes. In fact, as shown in Figure 5b, the fluorescence intensity decay was fitted with a monoexponential function with a half-time of ≈ 65 min. Moreover, the asymptotic limit fluorescence intensity at infinite time is zero, suggesting that over time all bacterial cells are permeabilized by the peptide. The slow decrease of the fluorescence intensity observed in Figure 5b might be dictated by slow diffusion caused by the electrostatic interactions between the cationic peptide and the anionic EPS matrix in addition to molecular sieving imposed by the macromolecular meshing in the matrix. Furthermore, an estimate for the diffusion coefficient of the peptide was calculated using the Brownian motion model for mean squared displacement: $D=7.2 \times 10^{-3} \mu\text{m}^2 \text{s}^{-1}$. A similar result has been reported for the linear viral-derived peptide pepR³⁹ ($D=4.5 \times 10^{-3} \mu\text{m}^2 \text{s}^{-1}$), in which such slow diffusion along the biofilm structure was ascribed to medium viscosity and electrostatic interactions with the biofilm matrix.

Conclusions

The antimicrobial activity of the spider-derived AMP gomesin, and its cyclic analogues, has been studied previously against bacteria in the planktonic form. Here, we report for the first time the activity of a gomesin-related peptide against bacterial biofilms, and demonstrate the potential of the designed cyclic analogue, [G1K,K8R]cGm, as a drug lead to fight bacterial biofilms. [G1K,K8R]cGm is known for its potent activity against bacteria in the planktonic form, high stability in serum and low toxicity to human

RBCs³². In the current study we show that it also displays potent activity against *S. aureus* biofilms by killing biofilm-embedded bacterial cells. The peptide was found to be more active than other β -hairpin peptides such as tachyplesin I–III and their cyclic analogues.⁵³ We also found that the 3D structure of [G1K,K8R] cGm is essential for its antibacterial and antibiofilm activities. Mechanistic studies suggest that the peptide can diffuse across the biofilm and kill bacteria by targeting and disrupting their cell membranes (Figure 6). AMPs able to reach bacteria within a complex polymeric matrix and kill them using a mechanism independent of their metabolic activity are an alternative approach to fight biofilm infections. Moreover, as recently shown for a cyclic analogue of the host-defence peptide IDR-108,⁵⁴ cyclic and disulphide-rich AMPs have additional advantages as they are likely to have improved resistance to proteolytic degradation and prolonged biological activity *in vivo*, compared to linear analogues.

Funding

This project received funding from the European Union's Horizon 2020 research and innovation programme under grant agreement No. 828774. This work was supported by project grants funded by Fundação para a Ciência e a Tecnologia (FCT-MCTES, Portugal; UIDB/04565/2020 and PPBI-POCI-01-0145-FEDER-022122). S.A.D. acknowledges FCT for the fellowship PD/BD/114425/2016. S.T.H. is an Australian Research Council (ARC) Future Fellow (FT150100398) and is supported by the ARC Centre of Excellence for Innovations in Peptide & Protein Science (CE200100012).

Transparency declarations

None to declare.

Supplementary data

Supplementary Methods, Tables S1 and Figures S1 to S3 are available as Supplementary data at JAC Online.

References

- Costerton JW, Stewart PS, Greenberg EP. Bacterial biofilms: a common cause of persistent infections. *Science* 1999; **284**: 1318–22. <https://doi.org/10.1126/science.284.5418.1318>
- Flemming HC, Wingender J. The biofilm matrix. *Nat Rev Microbiol* 2010; **8**: 623–33. <https://doi.org/10.1038/nrmicro2415>
- Davies D. Understanding biofilm resistance to antibacterial agents. *Nat Rev Drug Discov* 2003; **2**: 114–22. <https://doi.org/10.1038/nrd1008>
- Hall-Stoodley L, Costerton JW, Stoodley P. Bacterial biofilms: From the natural environment to infectious diseases. *Nat Rev Microbiol* 2004; **2**: 95–108. <https://doi.org/10.1038/nrmicro821>
- Del Pozo JL. Biofilm-related disease. *Expert Rev Anti Infect Ther* 2018; **16**: 51–65. <https://doi.org/10.1080/14787210.2018.1417036>
- Donlan RM. Biofilms and device-associated infections. *Emerg Infect Dis* 2001; **7**: 277–81. <https://doi.org/10.3201/eid0702.010226>
- Vertes A, Hitchins V, Phillips KS. Analytical challenges of microbial biofilms on medical devices. *Anal Chem* 2012; **84**: 3858–66. <https://doi.org/10.1021/ac2029997>
- Stempel N, Strehmel J, Overhage J. Potential application of antimicrobial peptides in the treatment of bacterial biofilm infections. *Curr Pharm Des* 2015; **21**: 67–84. <https://doi.org/10.2174/1381612820666140905124312>
- Di Luca M, Maccari G, Nifosi R. Treatment of microbial biofilms in the post-antibiotic era: prophylactic and therapeutic use of antimicrobial peptides and their design by bioinformatics tools. *Pathog Dis* 2014; **70**: 257–70. <https://doi.org/10.1111/2049-632X.12151>
- Hancock REW. Cationic peptides: effectors in innate immunity and novel antimicrobials. *Lancet Infect Dis* 2001; **1**: 156–64. [https://doi.org/10.1016/S1473-3099\(01\)00092-5](https://doi.org/10.1016/S1473-3099(01)00092-5)
- Bahar AA, Ren D. Antimicrobial peptides. *Pharmaceuticals* 2013; **6**: 1543–75. <https://doi.org/10.3390/ph6121543>
- Mahlapuu M, Håkansson J, Ringstad L et al. Antimicrobial peptides: an emerging category of therapeutic agents. *Agents Front Cell Infect Microbiol* 2016; **6**: 194.
- Silva PI, Daffre S, Bulet P. Isolation and characterization of gomesin, an 18-residue cysteine-rich defense peptide from the spider *Acanthoscurria gomesiana* hemocytes with sequence similarities to horseshoe crab antimicrobial peptides of the tachyplesin family. *J Biol Chem* 2000; **275**: 33464–70. <https://doi.org/10.1074/jbc.M001491200>
- Mandard N, Bulet P, Caille A et al. The solution structure of gomesin, an antimicrobial cysteine-rich peptide from the spider. *Eur J Biochem* 2002; **269**: 1190–8. <https://doi.org/10.1046/j.0014-2956.2002.02760.x>
- Machado A, Fázio MA, Miranda A et al. Synthesis and properties of cyclic gomesin and analogues. *J Pept Sci* 2012; **18**: 588–98. <https://doi.org/10.1002/psc.2439>
- Fázio MA, Oliveira VX, Bulet P et al. Structure-activity relationship studies of gomesin: importance of the disulfide bridges for conformation, bioactivities, and serum stability. *Biopolymers* 2006; **84**: 205–18. <https://doi.org/10.1002/bip.20396>
- Rodrigues EG, Dobroff ASS, Cavarsan CF et al. Effective topical treatment of subcutaneous murine B16F10-Nex2 melanoma by the antimicrobial peptide gomesin. *Neoplasia* 2008; **10**: 61–8. <https://doi.org/10.1593/neo.07885>
- Moreira CK, Rodrigues FG, Ghosh A et al. Effect of the antimicrobial peptide gomesin against different life stages of *Plasmodium* spp. *Exp Parasitol* 2007; **116**: 346–53. <https://doi.org/10.1016/j.exppara.2007.01.022>
- Barbosa FM, Daffre S, Maldonado RA et al. Gomesin, a peptide produced by the spider *Acanthoscurria gomesiana*, is a potent anticryptococcal agent that acts in synergism with fluconazole. *FEMS Microbiol Lett* 2007; **274**: 279–86. <https://doi.org/10.1111/j.1574-6968.2007.00850.x>
- Schaeffer M, de Miranda A, Mottram JC et al. Differentiation of *Leishmania major* is impaired by over-expression of pyroglutamyl peptidase I. *Mol Biochem Parasitol* 2006; **150**: 318–29. <https://doi.org/10.1016/j.molbiopara.2006.09.004>
- Domingues TM, Riske KA, Miranda A. Revealing the lytic mechanism of the antimicrobial peptide gomesin by observing giant unilamellar vesicles. *Langmuir* 2010; **26**: 11077–84. <https://doi.org/10.1021/la100662a>
- Mattei B, Miranda A, Perez KR et al. Structure-activity relationship of the antimicrobial peptide gomesin: the role of peptide hydrophobicity in its interaction with model membranes. *Langmuir* 2014; **30**: 3513–21. <https://doi.org/10.1021/la500146j>
- Horton DA, Bourne GT, Smythe ML. Exploring privileged structures: the combinatorial synthesis of cyclic peptides. *J Comput Aided Mol Des* 2002; **16**: 415–30. <https://doi.org/10.1023/A:1020863921840>
- Edman P. Chemistry of amino acids and peptides. *Annu Rev Biochem* 1959; **28**: 69–96. <https://doi.org/10.1146/annurev.bi.28.070159.000441>
- Qian Z, Rhodes CA, McCroskey LC et al. Drug delivery enhancing the cell permeability and metabolic stability of peptidyl drugs by reversible bi-cyclization. *Angew Chem Int Ed* 2017; **56**: 1525–9. <https://doi.org/10.1002/anie.201610888>

- 26** Rubin S, Qvit N. Cyclic peptides for protein–protein interaction targets: applications to human disease. *Crit Rev Eukaryot Gene Expr* 2016; **26**: 199–221. <https://doi.org/10.1615/CritRevEukaryotGeneExpr.2016016525>
- 27** Barbosa SC, Nobre TM, Volpati D *et al.* The importance of cyclic structure for Labaditin on its antimicrobial activity against *Staphylococcus aureus*. *Colloids Surfaces B Biointerfaces* 2016; **148**: 453–9. <https://doi.org/10.1016/j.colsurfb.2016.09.017>
- 28** Mika JT, Moiset G, Cirac AD *et al.* Structural basis for the enhanced activity of cyclic antimicrobial peptides: the case of BPC194. *Biochim Biophys Acta* 2011; **1808**: 2197–205. <https://doi.org/10.1016/j.bbame.2011.05.001>
- 29** Dathe M, Nikolenko H, Klose J *et al.* Cyclization increases the antimicrobial activity and selectivity of arginine- and tryptophan-containing hexapeptides. *Biochemistry* 2004; **43**: 9140–50. <https://doi.org/10.1021/bi035948v>
- 30** Garcia AE, Tai KP, Puttamadappa SS *et al.* Biosynthesis and antimicrobial evaluation of backbone-cyclized alpha-defensins. *Biochemistry* 2011; **50**: 10508–19. <https://doi.org/10.1021/bi201430f>
- 31** Chan LY, Zhang VM, Huang YH *et al.* Cyclization of the antimicrobial peptide Gomesin with native chemical ligation: influences on stability and bioactivity. *ChemBiochem* 2013; **14**: 617–24. <https://doi.org/10.1002/cbic.201300034>
- 32** Henriques ST, Lawrence N, Chaousis S *et al.* Redesigned spider peptide with improved antimicrobial and anticancer properties. *ACS Chem Biol* 2017; **12**: 2324–34. <https://doi.org/10.1021/acscchembio.7b00459>
- 33** Lebeaux D, Ghigo J-M, Beloin C. Biofilm-related infections: bridging the gap between clinical management and fundamental aspects of recalcitrance toward antibiotics. *Microbiol Mol Biol Rev* 2014; **78**: 510–43. <https://doi.org/10.1128/MMBR.00013-14>
- 34** Fisher RA, Gollan B, Helaine S. Persistent bacterial infections and persister cells. *Nat Rev Microbiol* 2017; **15**: 453–64. <https://doi.org/10.1038/nrmicro.2017.42>
- 35** Cheneval O, Schroeder CI, Durek T *et al.* Fmoc-based synthesis of disulfide-rich cyclic peptides. *J Org Chem* 2014; **79**: 5538–44. <https://doi.org/10.1021/jo500699m>
- 36** Wiegand I, Hilpert K, Hancock REW. Agar and broth dilution methods to determine the minimal inhibitory concentration (MIC) of antimicrobial substances. *Nat Protoc* 2008; **3**: 163–75. <https://doi.org/10.1038/nprot.2007.521>
- 37** CLSI. *Methods for Dilution Antimicrobial Susceptibility Tests for Bacteria That Grow Aerobically—Eleventh Edition: M07*. 2018.
- 38** Dias SA, Freire JM, Pérez-Peinado C *et al.* New potent membrane-targeting antibacterial peptides from viral capsid proteins. *Front Microbiol* 2017; **8**: 775.
- 39** Pinto SN, Dias SA, Cruz AF *et al.* The mechanism of action of pepR, a viral-derived peptide, against *Staphylococcus aureus* biofilms. *J Antimicrob Chemother* 2019; **74**: 2617–25. <https://doi.org/10.1093/jac/dkz223>
- 40** O'Brien J, Wilson I, Orton T *et al.* Investigation of the Alamar Blue (resazurin) fluorescent dye for the assessment of mammalian cell cytotoxicity. *Eur J Biochem* 2000; **267**: 5421–6. <https://doi.org/10.1046/j.1432-1327.2000.01606.x>
- 41** Mil-homens D, Fialho AM. A BCAM0223 mutant of *Burkholderia cenocepacia* is deficient in hemagglutination, serum resistance, adhesion to epithelial cells and virulence. *PLoS One* 2012; **7**: e41747. <https://doi.org/10.1371/journal.pone.0041747>
- 42** Pompilio A, Scocchi M, Pomponio S *et al.* Peptides antibacterial and anti-biofilm effects of cathelicidin peptides against pathogens isolated from cystic fibrosis patients. *Peptides* 2011; **32**: 1807–14. <https://doi.org/10.1016/j.peptides.2011.08.002>
- 43** Peeters E, Nelis HJ, Coenye T. Comparison of multiple methods for quantification of microbial biofilms grown in microtiter plates. *J Microbiol Methods* 2008; **72**: 157–65. <https://doi.org/10.1016/j.mimet.2007.11.010>
- 44** Chen HL, Su PY, Kuo SC *et al.* Adding a C-terminal cysteine (CTC) can enhance the bactericidal activity of three different antimicrobial peptides. *Front Microbiol* 2018; **9**: 1440. <https://doi.org/10.3389/fmicb.2018.01440>
- 45** Suthianthong P, Donpudsa S, Supungul P *et al.* The N-terminal glycine-rich and cysteine-rich regions are essential for antimicrobial activity of crustinPm1 from the black tiger shrimp *Penaeus monodon*. *Fish Shellfish Immunol* 2012; **33**: 977–83. <https://doi.org/10.1016/j.fsi.2012.08.010>
- 46** Conibear AC, Rosengren KJ, Daly NL *et al.* The cyclic cystine ladder in Θ -defensins is important for structure and stability, but not antibacterial activity. *J Biol Chem* 2013; **288**: 10830–40. <https://doi.org/10.1074/jbc.M113.451047>
- 47** Freudenthal O, Quiles F, Francius G. Discrepancies between cyclic and linear antimicrobial peptide actions on the spectrochemical and nanomechanical fingerprints of a young biofilm. *ACS Omega* 2017; **2**: 5861–72. <https://doi.org/10.1021/acsomega.7b00644>
- 48** Dufrière YF, Ando T, Garcia R *et al.* Imaging modes of atomic force microscopy for application in molecular and cell biology. *Nat Nanotechnol* 2017; **12**: 295–307. <https://doi.org/10.1038/nnano.2017.45>
- 49** Stiefel P, Schmidt-Emrich S, Maniura-Weber K *et al.* Critical aspects of using bacterial cell viability assays with the fluorophores SYTO9 and propidium iodide. *BMC Microbiol* 2015; **15**: 36. <https://doi.org/10.1186/s12866-015-0376-x>
- 50** Kerstens M, Boulet G, Tritsmans C *et al.* Flow cytometric enumeration of bacteria using TO-PRO[®]-3 iodide as a single-stain viability dye. *J Lab Autom* 2014; **19**: 555–61. <https://doi.org/10.1177/2211068214546745>
- 51** Davison WM, Pitts B, Stewart PS. Spatial and temporal patterns of bio-cide action against *Staphylococcus epidermidis* biofilms. *Antimicrob Agents Chemother* 2010; **54**: 2920–7. <https://doi.org/10.1128/AAC.01734-09>
- 52** Miles FL, Lynch JE, Sikes RA. Cell-based assays using calcein acetoxymethyl ester show variation in fluorescence with treatment conditions. *J Biol Methods* 2015; **2**: e29. <https://doi.org/10.14440/jbm.2015.73>
- 53** Vernen F, Harvey PJ, Dias SA *et al.* Characterization of tachyplesin peptides and their cyclized analogues to improve antimicrobial and anticancer properties. *Int J Mol Sci* 2019; **20**: 4184. <https://doi.org/10.3390/ijms20174184>
- 54** Etayash H, Pletzer D, Kumar P *et al.* Cyclic derivative of host-defense peptide IDR-1018 improves proteolytic stability, suppresses inflammation, and enhances in vivo activity. *J Med Chem* 2020; **63**: 9228–36. <https://doi.org/10.1021/acs.jmedchem.0c00303>